Single Stranded Breaks Relax Intrinsic Curvature in DNA

Dimitri E. Kamashev
CNRS UPR9051, Hôpital St. Lois, 1 av. C. Vellefaux, 75475 Paris Cedex 10, France.

Alexey K. Mazur*
Laboratoire de Biochimie Théorique, CNRS UPR9080,
Institut de Biologie Physico-Chimique, 13, rue Pierre et Marie Curie, Paris,75005, France

The macroscopic curvature of double helical DNA induced by regularly repeated adenine tracts (A-tracts) is well-known but still puzzling. Its physical origin remains controversial even though it is perhaps the best-documented sequence modulation of DNA structure. The recently proposed compressed backbone theory (CBT) suggested that the bending can result from a geometric mismatch between the specific backbone length and optimal base stacking orientations in B-DNA. It predicted that the curvature in A-tract repeats can be relaxed by introducing single stranded breaks (nicks). This effect have not been tested earlier and it would not be accounted for by alternative models of DNA bending. This paper checks the above prediction in a combined theoretical and experimental investigation. A series of nicked DNA fragments was constructed from two mother sequences with identical base pair composition, one including A-tract repeats and the other being random. The curvature was tested experimentally by gel mobility assays and, simultaneously, by free molecular dynamics (MD) simulations. Single stranded breaks produce virtually no effect upon the gel mobility of the random sequence DNA. In contrast, for nicked A-tract fragments, a regular modulation of curvature is observed depending upon the position of the strand break with respect to the overall bend. As predicted by CBT, the curvature is reduced, with maximal relaxation observed when the nick occurs inside A-tracts. These experimental results are partially reproduced in MD simulations of nicked A-tract repeats. Analysis of computed curved DNA conformations reveals modulations of local backbone length as measured by distances between some sugar atoms, with maximal backbone compression in the narrowing of the minor groove inside A-tracts. The results lend additional support to CBT versus alternative mechanisms of intrinsic curvature in DNA.

I. INTRODUCTION

The intrinsic curvature in DNA was discovered about twenty years ago for regular repeats of A_nT_m, with $n+m>3$, called A-tracts[1,2,3]. Several profound reviews exist of the large volume of related data accumulated during the last decades[4,5,6,7,8,9]. Due to its outstanding role in genome functioning and a very controversial experimental behavior, the sequence dependent DNA bending continues to attract great attention. The hottest point of debates is the molecular mechanism of this phenomenon. Already in the seventies, it was realized that the DNA double helix is not a rigid cylinder, but is bendable depending upon direction and the base pair sequence[10,11]. By postulating that stacking in ApA steps is intrinsically non-parallel the wedge model predicted that A-tracts repeated in phase with the helical screw should bend DNA[12]. This proved true, but the model later appeared unsatisfactory. It turned out that X-ray DNA structures are often bent in random sequences whereas A-tracts are exceptionally straight[13,14,15]. With the growing number of sequences checked, non-zero wedges had to be introduced for all base pair steps[16,17,18], nevertheless, experimental counter-examples were eventually found where bending could not result from accumulation of wedges[19,20]. Several theories tried to reveal other physical factors involved in DNA bending along with base stacking. The most popular junction model proposed by the Crother's group[2,21] originated from an idea that a bend should occur when two different DNA forms are stacked[22]. If poly(dA).poly(dT) double helix had a special B' form as suggested by some data[23] the helical axis should be kinked when an A-tract is interrupted by a random sequence. Drew and Travers[24,25] apparently were the first to notice that narrowing of both DNA grooves at the inner edge of a bend is a necessary and sufficient condition of bending. They, and later Burkhoff and Tullius[26], considered the preference of narrow and wide minor groove profiles by certain sequences as the possible original cause of this effect. Similar ideas were considered within the context of the junction model[27]. In addition, the possible involvement of solvent counterions in DNA bending was discussed long ago[28], and it has been extensively studied in the recent years[29,30,31]. Detailed analyses of all these theories including comparison with experimental data can be found in the recent literature[8,9,32]. Here we note only that, in spite of all efforts, the controversies remain and continue to accumulate[33,34].

Conformational calculations were always intensively used for testing various hypothesis concerning DNA bending[11,21,35,36,37,38,39,40]. The progress in methodology of molecular dynamics (MD) simulations of nucleic acids[41] recently made possible realistic modeling of A-tract DNA fragments[27,42,43,44]. In straightforward simulations of bending, the initial straight symmetrical DNA is allowed to bend spontaneously with no extra forces applied, that is due to generic atom-atom interactions[27,32,42,45,46]. Such computational ex-

periments are very demanding because they involve relatively long DNA fragments and require multi-nanosecond (at least) trajectories to reveal reliable trends toward bent states. Nevertheless, for preselected A-tract sequences, it was possible to demonstrate spontaneous emergence of intrinsic curvature in the course of simulations as well as attracting character of bent states, which is necessary for static curvature. These simulations resulted in a new hypothesis of the physical origin of intrinsic curvature which we refer to as the compressed backbone theory (CBT)[32,45,46].

In a certain sense, the CBT continues the line of earlier views that attributed the origin of bending to the properties of the DNA backbone[24,25,26,27]. It postulates that the intrinsic curvature in B-DNA results from a geometric mismatch between the length of the sugar-phosphate backbone and the base pair stacking. Starting from the first published drawing of the double helix[47], its two backbone strands are viewed as regular spiral traces that wind along the surface of the cylindrical B-DNA core formed by stacked base pairs. Because regular spirals represent the shortest lines that join two points on a cylindrical surface, and because the backbone strands are covalently linked to bases, an ideal B-DNA can exist only if the average backbone length either matches exactly or is shorter than that dictated by the base pair stacking[45]. The CBT assumes the opposite. It postulates that, under physiological conditions, the equilibrium specific length of the B-DNA backbone, considered as a restrained polymer attached to a cylindrical surface, is slightly longer that in the canonical B-form. In physics, similar mismatching relationship is often called geometric frustration[48]. The backbone tries to expand and "pushes" stacked bases while the stacking interactions oppose this. Eventually, the backbone finds a "compromise" by deviating from its regular spiral trace, which causes quasi-sinusoidal modulations of the DNA grooves. Concomitant base stacking perturbations cause local bends that accumulate to macroscopic static curvature when the period of these modulations corresponds to an integral number of helical turns. The CBT considers B-DNA double helices with any sequences and it may have a number of interesting consequences. It suggests, for example, that, even under normal temperature, the B-DNA double helix can occur in a glass-like state characterized by very long relaxation times[32]. The latter prediction agrees with some recent experimental data[49,50,51]. Under certain assumptions, one can even imagine the possibility of a glass-like aging of a single DNA molecule *in vivo*, with direct relation to the problems of biological aging.

One of the possible experimental tests of CBT is based upon the predicted effect of single-stranded breaks (nicks) upon the intrinsic curvature[32]. Reversible single chain breaks in DNA occur during diverse biochemical processes, including general and site-specific recombination, replication, and DNA repair. Therefore, structural perturbations due to nicks and single-stranded "gaps" have been earlier characterized in a number experimental studies[52,53,54,55,56,57,58,59,60,61,62,63,64,65,66,67,68]. According to all these data, nicks perturb the free DNA very little. The corresponding X-ray structures[58] are straight and similar to those of intact duplexes with analogous sequences. This agrees with early physicochemical tests[52,53,54] as well as NMR studies in solution[56,57,65,66,67]. The main detectable effect of a nick is local melting or fraying, especially at low ionic strength, mild denaturating conditions, or elevated temperatures. This increases the isotropic flexibility of DNA and reduces its gel mobility[60,61,63,68]. In normal conditions the nick fraying is small and it almost undetectable below 10°C[61,68].

Based upon these experimental data and the earlier views of the origin of intrinsic curvature one should expect that nicks in phased A-tract sequences can either increase bending or have zero effect. The increase may be expected if the curvature is caused by external forces, as in electrostatic counterion models, because the flexible hinge at a nick can allow these forces to increase the bend angle in their direction. A zero effect is expected for the wedge and junction models because nicks arguably do not affect the A-tract structures[58] and do not cause wedges detectable in gel migration assays[61]. In contrast, if the intrinsic curvature is really caused by the backbone compression, single-stranded breaks should relax it, which should increase the gel mobility of curved DNA fragments. This effect is opposite to that of the increased isotropic flexibility, moreover, the latter can be eliminated by reducing the temperature so that these two phenomena cannot be confused. In addition, because the degree of the compression should vary regularly between the inner and outer edges of the bent DNA, relaxation produced by a single nick is expected to change systematically according to its position with respect to the overall bend.

Here we present the results of experimental and simulation studies carried out according to the above plan. Two 35-mer sequences from our recent comparative investigation[32] were used for constructing two series of nicked DNA fragments. The first sequence contained an A-tract repeat motif that was preselected in MD simulations to reproducibly induce strong static curvature. The second sequence was “random”, but with the same base pair composition. Backbone breaks were introduced in one strand at different portions to span approximately one helical turn. The curvature was probed by PAGE as well as long-time MD simulations. In experiment, a noticeable increase in the gel mobility of the nicked A-tract repeat is observed depending upon the nick position. In contrast, no such effect is found for the random fragment. MD simulations fail to reproduce experimental effects qualitatively, but qualitatively they also confirm that single stranded breaks interfere with the A-tract induced curvature. The results qualitatively agree with CBT, but they cannot be accounted for by other models.

II. MATERIALS AND METHODS

A. Oligonucleotides and construction of 5'-labeled DNA probes

The double stranded DNA containing four A-tracts flanked poly(dA).poly(dT) termini were constructed by annealing the synthetic oligonucleotide B (the top line in Table I) with its complementary (bottom) strand. Double stranded DNA fragments containing single stranded breaks (nicks) were constructed by annealing two shorter oligonucleotides (Table I) with the same bottom strand. In the same way a series of nicked duplexes was constructed from the reference random sequence fragment S, with its base pair composition identical to that of B. The sequences of the oligonucleotides used for the construction of the DNA fragments are assembled in Table I. The fragment codes in this table use the following mnemonics. The capital 'B' and 'S' stand for "bent" and "straight". The small letter prefix 'n' stands for "nick". The numbers indicate the shift of the nick position with respect to the center of the sequence.

In all the constructs, one of the oligonucleotides annealed was labeled with T4 polynucleotide kinase and [^{32}-P]-ATP. In most cases the label was attached to the 5'-end of the bottom (continuous) oligonucleotide whereas the two strands at the nick position were terminated with 3'OH and 5'OH groups. For some sequences, 5'-phosphorylated nicks were additionally constructed to check the effect of phosphate charges. In this case the continuous strand carried 5'-OH while [^{32}-P] was introduced in the corresponding shorter partner. The annealing was carried out by incubating 300 nM of the unlabeled oligonucleotide(s) with 30 nM of end-labeled ones for 3 min at 80°C in 20 mM Tris-HCl (pH 8.0), 150 mM NaCl, and then allowing them to cool slowly. To distinguish between the two nick series, in the text, we add small letter suffixes 'o' and 'p' to the codes given in Table I. Thus the whole two nick series of the bent DNA are referred to as nBo and nBp, respectively, while the individual nicked fragments are denoted as nB-2o, nB-2p, etc.

B. Gel mobility assays

The mobility of the DNA fragments was analyzed in 12% gels (acrylamide to bis-acrylamide, 29:1) buffered with 90 mM Tris-borate, 1 mM EDTA, pH 8.6. In order to check the effect of Mg^{2+} ions the buffer was supplemented with 10 mM $MgCl_2$ in the absence of EDTA. Gels were pre-run under constant power until stabilization of the current. Labeled DNA in a buffer containing 20 mM Tris-HCl (pH 8.0), 50 mM NaCl, 4% Phicoll-400 and xylencianol was loaded onto the gel. The electrophoresis was performed under constant voltage and constant temperature of 4°C. The dried gels were exposed to storage phosphor screens and visualized on a 400S PhosphorImager (Molecular Dynamics).

C. Calculations

MD simulations were carried out for the central 35 base pairs of six nicked DNA fragments in Table I constructed from the A-tract repeat sequence (nB-4o, ..., nB+6o). The corresponding calculations for the two mother fragments without nicks (B and S) were reported earlier[32]. For consistency with the previous studies[32,45,46], we used the AMBER98[69,70] force field and TIP3P water[71]. Trajectories generally started from the fiber canonical B-DNA conformation[72] and were continued to 20 ns. In a few cases, dynamics was also run starting from the canonical A-DNA conformation. In total, these simulations sampled from more than 0.2 ms of all-atom dynamics for nicked and intact 35-mer DNA fragments with the same A-tract repeat sequence.

Molecular dynamics simulations were carried out with the internal coordinate molecular dynamics (ICMD) method[73,74] adapted for DNA[75,76] with the time step of 0.01 ps. In this approach, the DNA molecule has all bond length and almost all bond angles fixed at their standard values. The only variable bond angles are those centered at the sugar C1',...,C4', and O4' atoms, which assures the flexibility of the furanose rings. In contrast, bases, thymine methyls, and phosphate groups move as articulated rigid bodies, with only rotations around single bonds allowed. The highest frequencies in thus obtained models are additionally balanced by increasing rotational inertia of the lightest rigid bodies as described earlier[75,77]. The possible physical effects of the above modifications have been discussed elsewhere[74,78].

The so-called "minimal model" of B-DNA was used[75,79]. It includes only a partial hydration shell and treats counterion and long range solvation effects implicitly by reducing phosphate charges to -0.5 and applying linear scaling of Coulomb forces. This model produces B-DNA structures very close to experimental data and has no other bias towards bent or non-bent conformations except the base pair sequence. The interest to implicit solvation in DNA simulations is long standing and it continues in the literature[80]. Advantages as well as limitations of such approaches have been recently reviewed[41].

The minimal model is not meant to be generally applicable and we have chosen it for the present studies because of the following considerations. We assume that effects it ignores, like sequence specific counterion binding, play some role, but are not critical for the A-tract induced curvature. We have shown earlier that, in these conditions, the A-tract repeat motif we are using has a bent state with very strong attracting properties that allow one to observe spontaneous transitions to stable bent conformations in the course of MD[32,45]. This property is rather exceptional and only due to it one could hope to obtain useful information from a comparison between nicked and intact DNA in MD. We also carried out sev-

TABLE I: Construction of DNA fragments. A-tracts are boldfaced and nick positions are marked by double quotes.

Code	Sequence
B	A_{18}-**AAAAT**AGGCT**ATTTT**AGGCT**ATTTT**AGGCT**ATTTT**-T_{18}
nB-9	A_{18}-**AAAAT**AGG"CT**ATTTT**AGGCT**ATTTT**AGGCT**ATTTT**-T_{18}
nB-6	A_{18}-**AAAAT**AGGCT**A"TTTT**AGGCT**ATTTT**AGGCT**ATTTT**-T_{18}
nB-4	A_{18}-**AAAAT**AGGCT**ATT"TT**AGGCT**ATTTT**AGGCT**ATTTT**-T_{18}
nB-2	A_{18}-**AAAAT**AGGCT**ATTTT**"AGGCT**ATTTT**AGGCT**ATTTT**-T_{18}
nB+0	A_{18}-**AAAAT**AGGCT**ATTTT**AG"GCT**ATTTT**AGGCT**ATTTT**-T_{18}
nB+2	A_{18}-**AAAAT**AGGCT**ATTTT**AGGC"T**ATTTT**AGGCT**ATTTT**-T_{18}
nB+4	A_{18}-**AAAAT**AGGCT**ATTTT**AGGCT**A"TTTT**AGGCT**ATTTT**-T_{18}
nB+6	A_{18}-**AAAAT**AGGCT**ATTTT**AGGCT**ATT"TT**AGGCT**ATTTT**-T_{18}
nB+11	A_{18}-**AAAAT**AGGCT**ATTTT**AGGCT**ATTTT**AGG"CT**ATTTT**-T_{18}
S	A_{18}-TTAGATAGTATGACTATCTATGATCATGTATGATA-T_{18}
nS-9	A_{18}-TTAGATAG"TATGACTATCTATGATCATGTATGATA-T_{18}
nS-6	A_{18}-TTAGATAGTAT"GACTATCTATGATCATGTATGATA-T_{18}
nS-4	A_{18}-TTAGATAGTATGA"CTATCTATGATCATGTATGATA-T_{18}
nS-2	A_{18}-TTAGATAGTATGACT"ATCTATGATCATGTATGATA-T_{18}
nS+0	A_{18}-TTAGATAGTATGACTAT"CTATGATCATGTATGATA-T_{18}
nS+2	A_{18}-TTAGATAGTATGACTATCT"ATGATCATGTATGATA-T_{18}
nS+4	A_{18}-TTAGATAGTATGACTATCTAT"GATCATGTATGATA-T_{18}
nS+6	A_{18}-TTAGATAGTATGACTATCTATGA"TCATGTATGATA-T_{18}
nS+11	A_{18}-TTAGATAGTATGACTATCTATGATCATG"TATGATA-T_{18}

eral simulations for the mother 35-mer and 25-mer A-tract fragments by the Particle-Mesh Ewald method[81] with full solvation and periodical boundaries. The corresponding trajectories were continued to 5-10 ns, but they showed much less demonstrative bending dynamics. The origin of this difficulty is currently unclear, but it agrees with recent reports by some other authors[82]. Finally, the minimal model provides for substantial savings in computations. The saving factor is critical because DNA bending is detectable only in relatively long fragments and it is likely to involve very slow motions. In spite of a few reported analogous simulations using full-scale solvation[27,42] such calculations would be too costly for the volume of sampling reached here.

III. RESULTS AND DISCUSSION

A. Construction of DNA Fragments

The A-tract motif AAAATAG originally attracted our attention in MD simulations of the natural DNA fragment taken from the first curved DNA locus studied *in vitro*[2,46]. The central 35-mer A-tract repeat for the bent fragments in Table I was constructed by repeating this motif four times and it had to be inverted to make the two DNA termini symmetrical. Such inversion should not affect bending,[83] but is essential for simulations because the 3'- and 5'-end A-tracts may represent qualitatively different boundaries. In repeated simulations with this and similar A-tract fragments, the static curvature emerged spontaneously and it became more evident as the chain length increased[32,45]. To obtain a reference non-A-tract DNA, we have re-shuffled manually base pairs of the A-tract repeat. We preferred this randomized sequence to commonly used GC-rich straight fragments in order to keep the base pair content identical and reduce the noise that could cause small variations in gel mobility. In order to amplify the PAGE resolution of similarly bent nicked DNA, the 35-mer fragments were extended to 71 bp by adding poly(dA).poly(dT) tails. The tails continue the mother 35-mer A-tract repeat sequence smoothly, which should reduce the possible perturbations that could affect the comparison of PAGE results with MD simulations that involved only the central 35-mer nicked fragments.

B. Relative PAGE Mobilities

A representative PAGE plate of the random sequence series of non-phosphorylated nicks is shown in Fig. 1. All nicked DNA exhibit similar mobilities close to that of the reference straight fragment. A weak retardation effect distinguishable for some nick positions is at the limit of experimental accuracy. Qualitatively similar patterns, but with stronger retardation were earlier reported for nicked DNA fragments under elevated temperature and/or mild denaturating conditions[60,61,68]. We suppose, therefore, that some reduction of mobility in Fig. 1 results from the isotropic flexibility at nick positions that is strongly reduced at 4°C. This small retardation should be taken into account in the interpretation of other tests below.

Fig. 2 shows the results obtained in the same conditions for the A-tract nicks. The pattern exhibited here is evidently more complex than that in Fig. 1. On the one hand, for the central nick positions, the mobilities

FIG. 1: PAGE analysis of comparative mobilities of nicked DNA constructed from the random fragment. The contents of the lanes is as follows (see Table I and Methods for fragment codes). The lanes marked 'R' ("reference") contain a mixture of intact duplexes S and B. The series of lanes '-6', ..., '+6' contain nS-6o, ..., nS+6o, respectively.

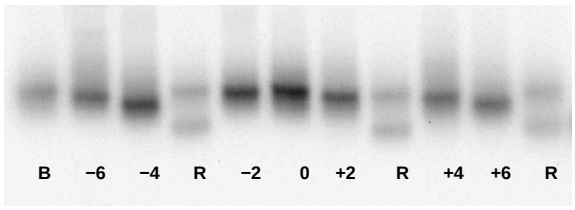

FIG. 2: PAGE analysis of comparative mobilities of nicked DNA constructed from the A-tract repeat fragment. The contents of the lanes is as follows (see Table I and Methods for fragment codes). The lanes marked 'B' and 'R' ("reference") contain the intact B and its mixture with S, respectively. The series of lanes '-6', ..., '+6' contain nB-6o, ..., nB+6o, respectively.

are close to that of the mother fragment, which is qualitatively similar to Fig. 1. However, when the nick is moved farther from the center, the PAGE mobility grows and becomes higher than that of the mother curved fragment. It reaches maximum values for nB-4o and nB+6o, but for nB-6o it is reduced again. As a result, the mobilities of nB-6o and nB-4o appear close to those of nB+4o and nB+4o, respectively, and the overall pattern of nick bands in Fig. 2 appears skewed-sinusoidal, with the period corresponding to that of the double helix. The increase of PAGE mobility indicates reduced DNA curvature and this effect can well be due to the relaxation predicted by CBT. The amplitude of the reduction is very significant since it exceeds 30% of the curvature difference between the S and B fragments produced by four A-tracts. This mobility profile suggests that the backbone compression is maximal within A-tracts and minimal between them. Although this specific phasing is right opposite to our first guess[32] it is accounted for by CBT and not by other theories as we discuss further below. However, there are a few alternative interpretations that should be considered first.

The first evident factor that should be checked is the perturbed balance of phosphate charges. The two nick series displayed in Fig. 1 and Fig. 2 have one phosphate group less than the reference fragments B and S. Consequently, their mobilities may be uniformly reduced by around 0.7%, which would mean that the apparent reduction of curvature in the nicked A-tract fragments nB-4o and nB+6o is even stronger than it is seems from Fig. 2. This effect, however, is not distinguishable in Fig. 1 suggesting that it is too small and may be safely neglected. The influence of phosphate charges can be more subtle, however. The electrostatic models of DNA bending assume that it is the broken balance of phosphate repulsion at the opposite DNA sides that forces it to bend[31]. If the A-tract curvature had an electrostatic origin, the phosphate "hole" at the nick could perturb it by adding a local bend in a direction that should rotate as the "hole" is moved along the DNA chain. Like that the integral curvature would be deviated and partially compensated in a way compatible with the results shown in Fig. 2.

To check this possibility, similar experiments were carried out for a series of analogous phosphorylated nicks. Their relative PAGE mobilities are compared with other results in Fig. 3. The mobility coefficients Q_m used in this plate were computed as follows. The Q_m value of the S fragment (see Table I) is always the largest in the gel and it is arbitrarily assumed to equal 100. The Q_m of fragment B is assumed to equal 0. For any given band its Q_m is promotional to the distance from the fastest S band in the same gel and it is estimated relative to the distance between B and S. If a nicked fragment migrates slower than the B-band in the same gel its Q_m is negative. In contrast, if it is faster, the corresponding Q_m is positive below 100. Fig. 3 displays thus obtained Q_m values for all DNA fragments used in the present study.

With free 5'-phosphates added to the nick sites, the phosphate "holes" are quenched or even inverted, which should drastically change the observed curvature modulations. The results in Fig. 3, however, show the oppo-

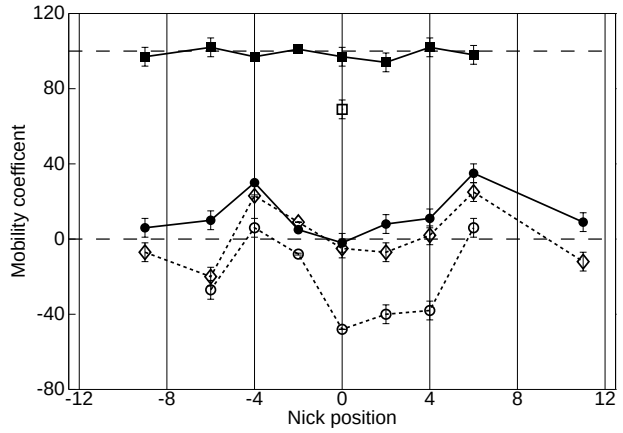

FIG. 3: Quantitative comparison of relative mobilities of DNA fragments listed in Table I. The method of calculation of the mobility coefficients Q_m is explained in the text. The reference mobilities of fragments B and S are indicated by horizontal dashed lines. The error bars indicate the estimate of experimental errors obtained from variation of Q_m in repeated runs.

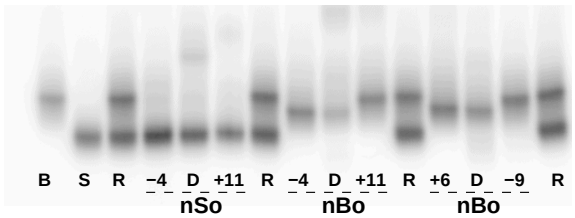

FIG. 4: PAGE analysis of comparative mobilities of double nicked DNA constructed from the random and A-tract repeat fragments. The contents of the lanes is as follows (see Table I and Methods for fragment codes). The lanes marked 'S,', 'B' and 'R' ("reference") contain the intact fragments S, B, and their mixture, respectively. Lanes marked by integer numbers contain the corresponding single-nicked DNA fragments of the series marked below. Lanes marked 'D' contain DNA fragments carrying simultaneously the two nicks from the left and right neighbor lanes.

site. The original skewed-sinusoidal dependence is persistent. At the same time, the phosphorylated nicks exhibit uniformly reduced mobilities, which agrees with earlier reports[60,61] and should be attributed to the increased strand fraying in nicks. The additional phosphate charge increases the inter-strand electrostatic repulsion at single stranded breaks, which should enhance the fraying effect as discussed in detail elsewhere[63]. Whatever the reason of the uniformly reduced mobility, however, Fig. 3 clearly shows that the above hypothesis of electrostatic curvature compensation can be ruled out.

This figure also shows the profile of mobilities of the nBo series in the presence of Mg^{2+} ions. The Mg^{2+} ions are long known to affect the DNA curvature by increasing or reducing it depending upon the sequence[84,85]. In our case the curvature was increased as judged from the absolute PAGE separation of fragments B and S. It is seen in Fig. 3 that the profile of the nick mobilities in the presence of Mg^{2+} ions remains qualitatively similar, but some nicks migrated slower than the mother B fragment. Interpretation of this effect depends upon the mechanism by which Mg^{2+} increase the A-tract curvature. If the additional bend is caused by the electrostatic attraction due to Mg^{2+} positioning between the phosphate groups in the narrowings of the major groove than the gain in the curvature may be larger when the DNA is nicked in the widening of the minor groove at the opposite side of the bend. This interpretation would agree with Fig. 3 because the negative Q_m are observed for nick positions outside A-tracts in the probable widenings of the minor groove. It is also possible, however, that Mg^{2+} ions somehow increase the nick fraying especially when the nick position approaches the poly(dA).poly(dT) tails. In this case, the negative Q_m values would have the same origin as for the phosphorylated nicks.

The results in Fig. 2 can also be interpreted with the wedge model of DNA bending by assuming that nicks have a special structure with a wedge in a fixed local direction. The overall curvature is reduced when this wedge direction is opposite to that of the initial bend and increased in the opposite orientation. Similarly to the "phosphate hole" model above, skewed-sinusoidal modulations of curvature should occur as the nick site is translated along DNA. Note that this wedge should have a very large angle since it compensates in nB-4o and nB+6o more than 30% of the curvature due to four phased A-tracts. A strong wedge like that should result in an increased curvature in nB+0o as well as in the nSo series in Fig. 1, which is not seen. This interpretation also would not agree with earlier studies of nick structures and gel mobilities[58,61,63]. However, earlier PAGE studies were carried out at higher temperatures where the isotropic flexibility of nicks could, in principle, dominate all other effects. Also, the non-linear dependence of the gel mobility upon the curvature may be such that the acceleration effect of the nick wedge in Fig. 2 is more pronounced than the expected retardation for nB+0o and the nSo series. Therefore, in order to check the above explanations, double nicked A-tract fragments were constructed, with the two sites separated by an odd number of helical half-turns so that the hypothetical wedges had opposite directions and should have compensated one another. The PAGE mobilities of double nicked fragments are compared in Fig. 4. These data evidently disagree with the foregoing wedge interpretation of mobility modulations. For both nB-4o and nB+6o, the addition of a second nick at 1.5 helical turn neither cancel nor even reduce the corresponding band shifts with respect to Fig. 2. As expected, analogous constructs for fragment S all show PAGE mobilities similar to that of the intact duplex.

The experimental results presented above evidence that single stranded breaks really reduce the overall cur-

TABLE II: Structural parameters of standard and computed DNA conformations. The top row features the canonical B-DNA values corresponding to the fiber crystal structure[72]. The RMSD values were computed with respect to this conformation. The results are shown for the last 1 ns averaged structures from the corresponding trajectories. The data for B and S trajectories are taken from our previous report[32]. The helicoidals are the sequence averaged values computed with program Curves[86]. All distances are in angströms and angles in degrees.

	Xdisp	Inclin	Rise	Twist	RMSD
B-DNA	-0.7	-6.0	3.4	36.0	0.0
S	-0.1	-4.7	3.5	34.4	4.1
B	-0.4	-4.0	3.5	34.2	6.8
nB-4o	-0.4	-3.3	3.5	34.7	6.0
nB-2o	-0.3	-3.4	3.5	34.5	3.2
nB+0o	-0.1	-5.0	3.5	34.5	6.4
nB+2o	-0.7	-4.4	3.5	34.1	4.0
nB+4o	-0.6	-4.5	3.5	34.1	3.3
nB+6o	-0.6	-4.3	3.5	34.3	4.8

TABLE III: Local inter-base parameters at strand breaks. The nicked steps only were analyzed with Curves[86] in the last five 1ns averaged structures. The same steps were analyzed in their intact states by similarly using the B trajectory of the mother A-tract fragment. Each fragment is characterized by two lines showing the averages and standard deviations for the given base step in its nicked (top) and intact (bottom) states. All distances are in angströms and angles in degrees.

Shift	Slide	Rise	Tilt	Roll	Twist
			nB − 4o		
1.2±0.3	-0.4±0.1	3.3±0.1	9.7±1.7	-14.6± 4.9	40.5±1.3
0.9±0.8	-0.7±0.2	3.2±0.2	7.8±2.7	-4.1± 5.1	37.5±5.8
			nB − 2o		
0.5±0.2	2.6±0.1	3.2±0.1	12.7±1.4	4.2± 3.0	7.8±2.9
1.2±0.9	0.1±0.2	3.2±0.2	10.3±3.4	5.8± 2.7	37.5±2.2
			nB + 0o		
-1.0±0.1	1.2±0.2	3.6±0.2	-11.1±6.5	1.8± 2.4	52.2±2.8
0.4±0.2	-1.2±0.2	3.5±0.1	0.7±1.0	-1.8± 2.7	32.6±1.0
			nB + 2o		
-0.9±0.1	-0.1±0.6	2.8±0.1	14.0±2.7	-2.3± 7.9	20.7±2.7
0.1±0.2	-1.8±0.1	3.8±0.1	-2.6±2.6	-3.8± 1.5	32.0±1.6
			nB + 4o		
-0.6±0.2	-1.3±0.2	3.3±0.2	5.3±2.8	-10.8±10.1	25.6±1.7
-0.2±0.1	-1.5±0.2	3.4±0.1	3.6±2.1	-10.3± 2.8	30.4±0.8
			nB + 6o		
0.8±0.1	-0.4±0.3	3.4±0.2	9.6±2.0	-23.9± 5.1	39.0±1.7
0.5±0.2	-1.1±0.2	3.4±0.2	3.7±3.0	-8.3± 1.2	37.0±2.1

vature of the A-tract repeat in remarkable qualitative agreement with CBT. Other theories of DNA bending cannot account for these data unless strong *ad hoc* assumptions are introduced like sequence-and-position dependent nick wedges, for example.

C. DNA Curvature in Simulations

As regards the overall stability of dynamics and its closeness to the B form, all MD trajectories computed in the course of this studies were similar to our earlier simulations under similar conditions[32,45,46,75,79]. Table II shows parameters of the final 1ns-average conformations. They all have remarkably similar average helicoidals corresponding to a typical B-DNA. For example, the average helical twist estimated from the best-fit B-DNA experimental values[87] gives $34.0 \pm 0.2^\circ$ and $33.8 \pm 0.2^\circ$ for the A-tract fragment and the randomized sequence, respectively. The nicks did not cause readily visible perturbations and it was commonly difficult to distinguish them in snapshots. Statistical analysis of the local inter-base parameters at nick positions is summarized in Table III. As expected, the broken DNA strand exhibits somewhat increased flexibility at the nick site. The most noticeable are much stronger deviations of Twist form its canonical values. A similar feature is smaller, but distinguishable for Tilt and Roll. On the other hand, the nanosecond time scale fluctuations characterized by the standard deviations are not very different with and without the nick. The last observation suggests that, as long as the bases at the nicked step remain in the stack, their rapid motions are restrained to the same degree as in the intact structure, and that the above strong deviations of some averages are due to slower global motions that occur in much longer time scales. Apart from these strong fluctuations, however, we did not observe any repetitive static perturbations that might be attributed to strand breaking. Moreover, strongly non-canonical helical parameters are sometimes encountered in intact steps as well. As it was for dynamics of the mother A-tract DNA fragment[32], the rms deviations from the canonical structures seen in Table II are largely due to variation of the overall curvature.

Fig. 5 compares the overall DNA curvature in the last five 1ns averaged conformations from all trajectories mentioned in Table II. It is seen that the mother A-tract fragment (B) reached the largest bending amplitudes non accessible to other fragments. The most stable and significant curvature among the nicks is obtained for nB-4o and nB+0o. Detailed in Fig. 6 is the dynamics of the bend direction. Its short time scale fluctuations are smaller when bending is strong, therefore, Fig. 6 also gives an estimate of the bending amplitude. Again we note that the mother A-tract fragment (B) is distinguished by the rapid establishment of curvature. However, convergence to a statically bent state is clear for nB-4o and nB+0o as well. Following to our previous approach[32,45,46] an attempt has been made to confirm the attracting property of the bent state for nB+0o by running dynamics starting from the canonical A-DNA conformation. The corresponding trajectory was continued to 17 ns and it showed convergence of the same bending direction as in Fig. 6, but with a somewhat smaller amplitude.

Fig. 5 and Fig. 6 show that our MD simulations failed

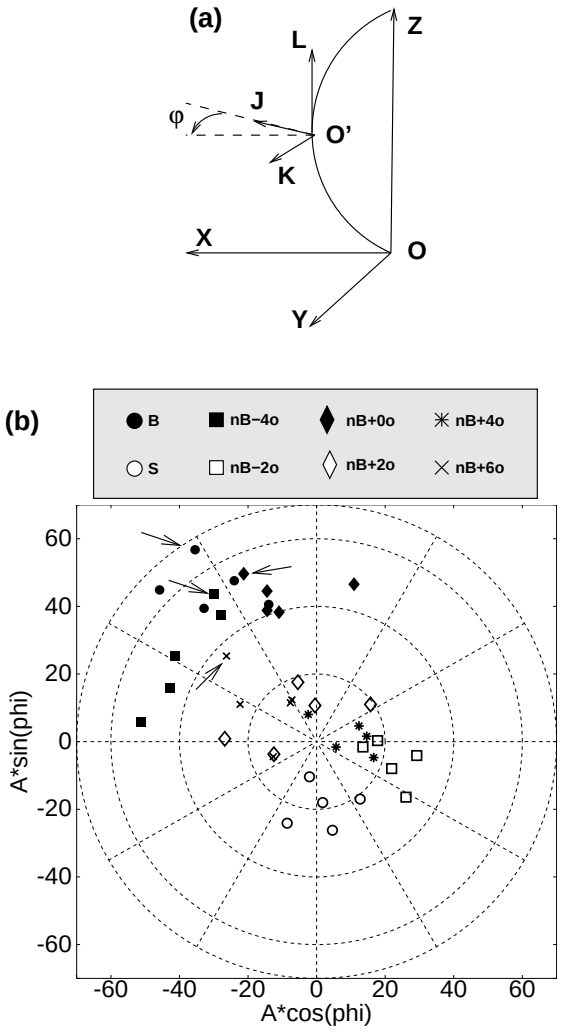

FIG. 5: (a) Geometric constructions used for evaluating the DNA bending. The amplitude of bending is measured by the angle between the ends of the curved helical axis produced by the Curves algorithm[86]. The two coordinate frames shown are the global Cartesian coordinates (OXYZ), and the local frame constructed in the middle point according to the Cambridge convention (O'JKL)[88]. The curve is rotated with two its ends fixed at the Z-axis to put the middle point in plane XOZ. The bending direction is measured by angle φ between this plane and vector **J** of the local frame. By definition, this vector points to the major DNA groove along the short axis of the reference base pair[88]. Consequently, the zero φ value corresponds to the overall bend towards the minor groove in the middle of the DNA fragment as it was in the very first analyses of local DNA curvature[11].
(b) Polar plot of bending angle (A) versus direction (phi). The results are shown for the last five 1 ns averaged structures from each trajectory, with the curvature measured as explained in plate (a).

to reproduce a regular variation of the bending magnitude with the nick position as seen in the PAGE experiments above. Fragments nB-4o and nB+0o exhibit noticeable curvature comparable, but smaller than that of the intact duplex. According to experiment, the curvature in nB+0o is similar to that in the mother fragment, but for nB-4o it should be definitely smaller. Fragment nB+6o exhibited less stable bending in a similar direction whereas for nB-2o, nB+2o, and nB+4o the 20 ns duration of trajectories apparently was not sufficient for convergence. At the same time, our calculations confirm that, in qualitative agreement with experiment, single strand breaking interferes with bending and generally reduces it. It is remarkable in Fig. 5 that strong bends beyond 40° were observed only in directions roughly corresponding to that in the mother fragment, which confirms the strong attracting property of this bent state. Taking into account the unclear physical nature of the phenomenon being studied and the complexity of the model system we consider the partial qualitative agreement achieved here as very satisfactory.

In spite of this only limited agreement with experiment, we tried to use the ensemble of computed curved DNA conformations to clarify the origin of the effect produced by nicks upon the A-tract curvature. To this end, for each of the fragments B, nB-4o, nB+0o, and nB+6o a nanosecond of dynamics have been selected for a more detailed analysis. The corresponding 1ns average structures are marked by arrows in Fig. 5. They all correspond to the largest degree of curvature reached during these trajectories. For B and nB+6o these are the last nanosecond structures. In contrast, for nB-4o and nB+0o the 17th and the 19th nanoseconds were used, respectively. According to Fig. 5, these bends are more or less convergent suggesting that the corresponding dynamics should be similar and subtle differences caused by nicks might be detectable. As seen in Fig. 7, for fragments B, nB-4o, and nB+6o the averaged conformations are rather close to one another. The curved DNA axis is almost planar with two or three zones of increased bending found between the A-tracts. In contrast, for nB+0o the curved axis is strongly non-planar due to significant deviation of bend direction in its central zone from the other two. As a result, for B, nB-4o, and nB+6o the overall bend is close to the sum of local bends, but for nB+Oo it is much smaller. The minor groove profiles averaged over the corresponding 1 ns periods are compared in Fig. 8. Again one can note a similarity between B, nB-4o, and nB+6o versus a more complex profile for nB+Oo. The widenings of the minor groove are found between A-tracts and they roughly correspond to the zones of increased bending in Fig. 7. According to Fig. 7 and Fig. 8, a reduced overall bending amplitude in nB-4o and nB+6o with respect to the mother A-tract fragment is attributable to the central zone where the widening is also less significant. In contrast, the smaller curvature in nB+0o is mainly due to the lost phasing between the local bends.

Relaxation of A-tract curvature by single stranded

breaks has been originally proposed as a conceptual test of CBT[32]. The results reported here qualitatively agree with its predictions and strongly support this model versus its alternatives. At the same time, the nick position dependence as revealed by our PAGE tests is inverted with respect to to the original guess[32]. We thought that the backbone compression is maximal in the widenings of the minor groove, therefore, nicks between A-tracts should relax bending stronger than nicks inside them. In contrast, the experiments reported above suggest that the backbone compression should increase inside A-tracts and reduce outside them. Because A-tracts are found at the internal edge of the curved double helix the last suggestion agrees with the simple physical intuition that says that the surface of a curved cylinder is compressed at its inner edge and stretched at the opposite side. In order to understand which backbone component can be responsible for the compression/frustration relationship postulated by CBT we tried to measure the specific backbone length by using pairs of similar atoms in neighboring residues.

For all atom pairs the resulting profiles of the backbone length appear very noisy and regular modulations can be seen only after averaging with a sliding window. Inspection of all atom pairs allows one to divide them in two groups. For atoms of phosphate groups and their neighbors, the measured backbone length usually is larger at the inner side of the bend and smaller at the opposite side, which may be viewed as a trend towards the A-from in the widenings of the major groove. However, these modulations are very weak, in agreement with the conventional view of the B-DNA backbone as being non-compressible[90,91]. In contrast, for a group of backbone atoms including O4' and its close neighbors, strong regular oscillations of the backbone length could be revealed, with their phases being opposite to those in the first group. The average backbone profiles produced by inter-O4' distances are shown in Fig. 9. They were computed for the 1 ns intervals of trajectories marked in Fig. 5. It is seen that the backbone length correlates with the minor groove profiles in Fig. 8, but does not repeat them. Thus measured specific backbone length reaches its local minima at the inner edge of the bent DNA cylinder and corresponds exactly to the nick positions in nB-4o and nB+6o. Similar oscillations are observed in X-ray structures of bent DNA available in NDB[92] (AKM, unpublished). It may seem surprising that profiles in Fig. 9 exhibit no perturbations at strand breaks, but this results from smoothing. In the non-smoothed plots the single stranded breaks in nB+6o and nB+0o were distinguished by very small and very large distances, respectively, but they have been compensated by strong opposite deviations in the neighboring steps.

The foregoing analysis demonstrates that the DNA backbone behaves as a complex mechanical system rather than a chain of strings or rigid rods, and that different its components compress and stretch in different zones of the curved DNA. Nevertheless, the correlations revealed in Fig. 9 suggest that the backbone compression, if it really exists, should mainly affect sugar-sugar interactions and that they can be at the origin of the intrinsic backbone frustration. Even though in B-DNA consecutive O4' atoms do not interact, the neighboring sugar rings make a number of direct contacts non-mediated by the solvent.

IV. CONCLUDING DISCUSSION

The results presented here provide new insights in the putative physical mechanism of intrinsic DNA curvature. This intriguing phenomenon seems to be exhaustively studied, but it still attracts great interest. The A-tract repeats and single stranded breaks both have been earlier recognized as elements specifically involved in DNA bending. To our best knowledge, however, nobody checked what could be their cumulative effect. Here it is found that nicks relax the intrinsic curvature induced by A-tract repeats in conditions where they do not affect the random sequence DNA. The relaxation effect depends upon the nick position with respect to the bend. It is very significant when the nick is at the inner edge of the bent DNA inside A-tracts, and is gradually reduced essentially to zero when the nick is moved to the outer surface of the bend. This behavior is in qualitative agreement with the CBT and it suggests that the backbone compression in the curved DNA is larger in the minor groove narrowings at the inner surface.

The MD simulations confirm that single stranded breaks interfere with, and tend to relax the A-tract induced curvature. For about a half of the DNA fragments studied, the duration of trajectories provided reproducible convergence to statically bent states in good agreement with experiment as well as earlier simulations. Inspection of the computed conformations reveals strong regular modulations of the local backbone length as measured by distances between certain sugar atoms, with compression reaching its maximum at the inner edge of the bend where nicks produce the strongest relaxation in experiments. These results provide additional support to the CBT and suggest that the frustration in the B-DNA backbone may result from interactions between consecutive sugar rings.

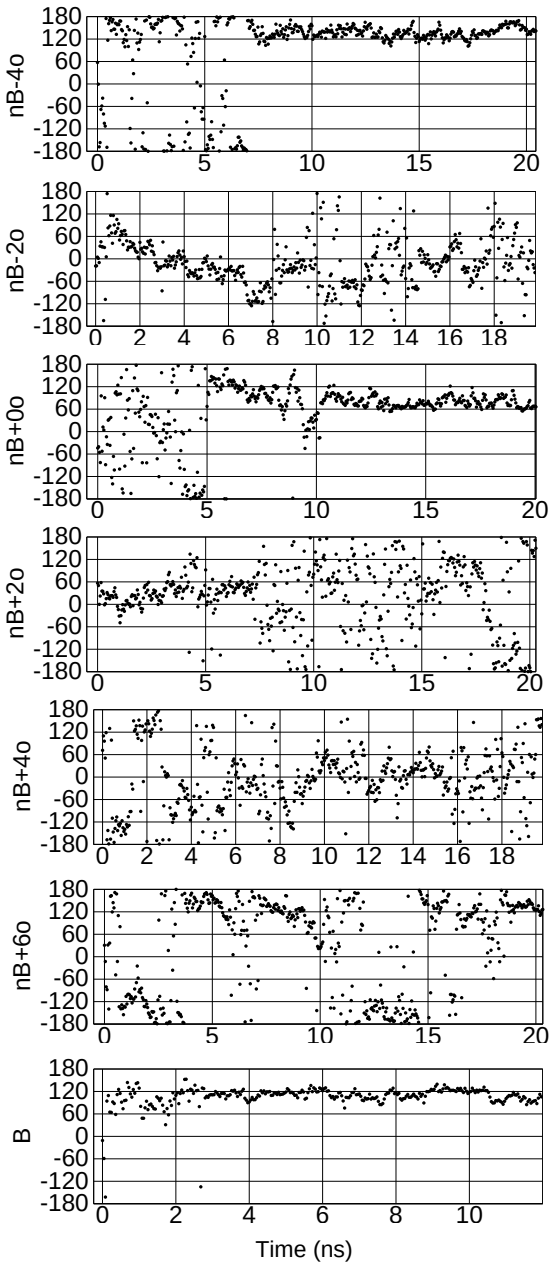

FIG. 6: The time evolution of the bending direction as measured by the φ angle in Fig. 5a (in degrees). Here the axis of the curved double helix was computed as the best fit common axis of coaxial cylindrical surfaces passing through sugar atoms, which gives solutions close to those produced by the Curves algorithm[86]. The traces have been smoothed by averaging with a window of 60 ps and are displayed with a time step of 40 ps.

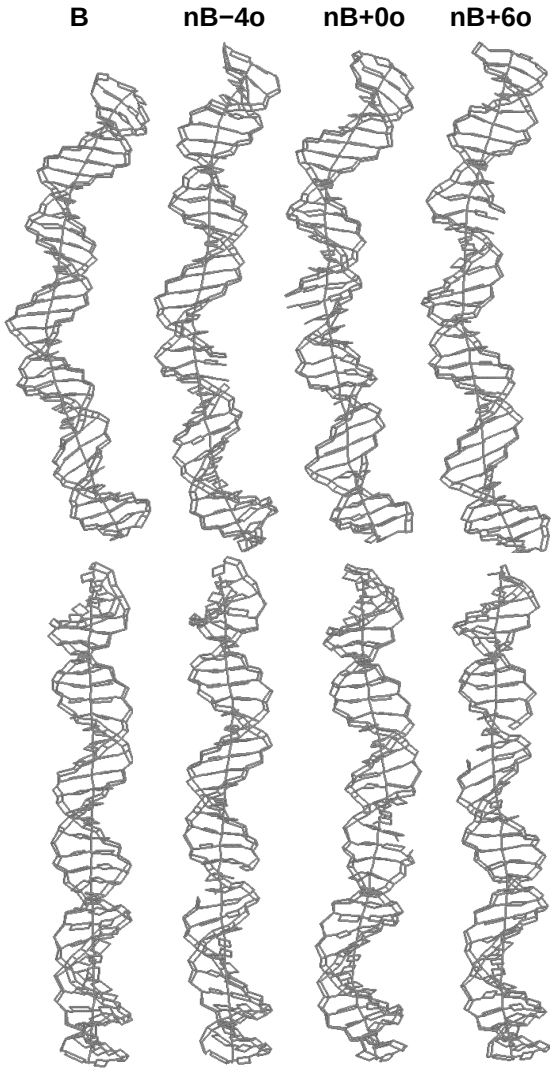

FIG. 7: Schematic drawings of the of 1 ns averaged structures marked by arrows in Fig. 5. The pictures were produced with Curves[86]. The backbone breaks are distinguished by three consecutive gaps in the ribbons, but only the central phosphate is in fact absent. Two orthogonal views are shown. The upper and lower views correspond to the negative direction of the OY axis and the positive direction of the OX axis, respectively, as shown in in Fig. 5a.

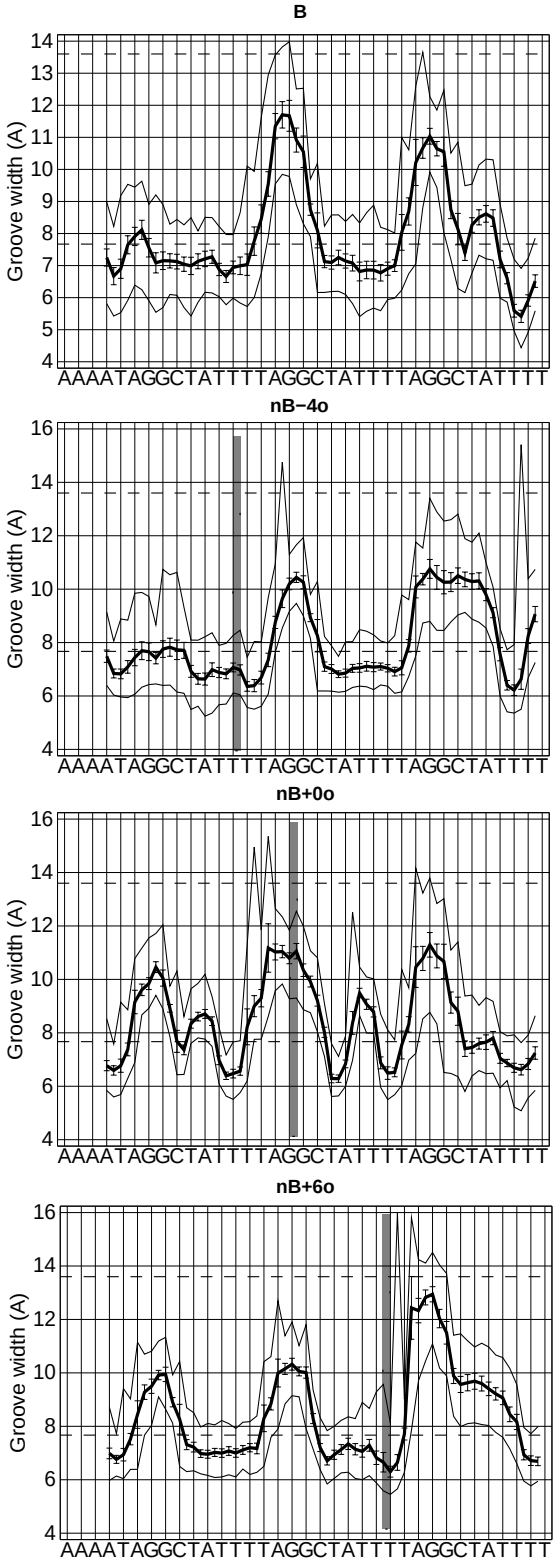

FIG. 8: The profiles of the minor groove profile averaged over the 1 ns trajectory intervals marked in Fig. 5. The central traces represent the average groove width with rms fluctuations shown as error bars. The upper and lower solid traces show the maximal and minimal values, respectively. The groove width is evaluated by using space traces of C5' atoms[89]. Its value is given in angströms, with the corresponding canonical A- and B-DNA levels indicated by the horizontal dashed lines. The vertical grey bars mark nick positions.

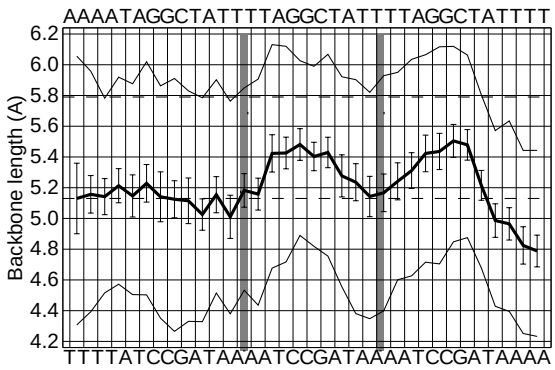

FIG. 9: Backbone length profiles averaged over the 1 ns trajectory intervals marked in Fig. 5. The plots were generated by using inter-O4' distances. The central traces represent the average with rms fluctuations shown as error bars. The upper and lower solid traces show the maximal and minimal values, respectively. All profiles were smoothed with a sliding window of 3 base pair steps. The length is given in angströms, with the corresponding canonical A- and B-DNA levels indicated by the horizontal dashed lines. The vertical grey bars mark nick positions.

* Electronic address: alexey@ibpc.fr; FAX:+33[0]1.58.41.50.26

[1] J. C. Marini, S. D. Levene, D. M. Crothers, and P. T. Englund, Proc. Natl. Acad. Sci. U.S.A. **79**, 7664 (1982).

[2] H.-M. Wu and D. M. Crothers, Nature **308**, 509 (1984).

[3] P. J. Hagerman, Proc. Natl. Acad. Sci. U.S.A. **81**, 4632 (1984).

[4] S. Diekmann, in *Nucleic Acids and Molecular Biology, Vol. 1*, edited by F. Eckstein and D. M. J. Lilley (Springer-Verlag, Berlin, 1987), pp. 138–156.

[5] P. J. Hagerman, Annu. Rev. Biochem. **59**, 755 (1990).

[6] D. M. Crothers, T. E. Haran, and J. G. Nadeau, J. Biol. Chem. **265**, 7093 (1990).

[7] D. M. Crothers and J. Drak, Methods Enzymol. **212**, 46 (1992).

[8] W. K. Olson and V. B. Zhurkin, in *Structure and Dynamics. Vol. 2: Proceedings of the Ninth Conversation, State University of New York, Albany, N.Y. 1995*, edited by R. H. Sarma and M. H. Sarma (Adenine Press, New York, 1996), pp. 341–370.

[9] D. M. Crothers and Z. Shakked, in *Oxford Handbook of Nucleic Acid Structure*, edited by S. Neidle (Oxford University Press, New York, 1999), pp. 455–470.

[10] N. Z. Namoradze, A. N. Goryunov, and T. M. Birshtein, Biophys. Chem. **7**, 59 (1977).

[11] V. B. Zhurkin, Y. P. Lysov, and V. I. Ivanov, Nucleic Acids Res. **6**, 1081 (1979).

[12] E. N. Trifonov and J. L. Sussman, Proc. Natl. Acad. Sci. U.S.A. **77**, 3816 (1980).

[13] C. R. Calladine, H. R. Drew, and M. J. McCall, J. Mol. Biol. **201**, 127 (1988).

[14] R. C. Maroun and W. K. Olson, Biopolymers **27**, 585 (1988).

[15] R. E. Dickerson, D. S. Goodsell, and S. Neidle, Proc. Natl. Acad. Sci. U.S.A. **91**, 3579 (1994).

[16] P. De Santis, A. Palleschi, M. Savino, and A. Scipioni, Biochemistry **29**, 9269 (1990).

[17] A. Bolshoy, P. McNamara, R. E. Harrington, and E. N. Trifonov, Proc. Natl. Acad. Sci. U.S.A. **88**, 2312 (1991).

[18] Y. Liu and D. L. Beveridge, J. Biomol. Struct. Dyn. **18**, 505 (2001).

[19] M. Dlakić and R. E. Harrington, Proc. Natl. Acad. Sci. U.S.A. **93**, 3847 (1996).

[20] M. Dlakić and R. E. Harrington, Nucleic Acids Res. **26**, 4274 (1998).

[21] S. D. Levene and D. M. Crothers, J. Biomol. Struct. Dyn. **1**, 429 (1983).

[22] E. Selsing, R. D. Wells, C. J. Alden, and S. Arnott, J. Biol. Chem. **254**, 5417 (1979).

[23] D. G. Alexeev, A. A. Lipanov, and I. Y. Skuratovskii, Nature **325**, 821 (1987).

[24] H. R. Drew and A. A. Travers, Cell **37**, 491 (1984).

[25] H. R. Drew and A. A. Travers, J. Mol. Biol. **186**, 773 (1985).

[26] A. M. Burkhoff and T. D. Tullius, Cell **48**, 935 (1987).

[27] D. Sprous, M. A. Young, and D. L. Beveridge, J. Mol. Biol. **285**, 1623 (1999).

[28] S. D. Levene, H.-M. Wu, and D. M. Crothers, Biochemistry **25**, 3988 (1986).

[29] M. A. Young, B. Jayaram, and D. L. Beveridge, J. Am. Chem. Soc. **119**, 59 (1997).

[30] I. Rouzina and V. A. Bloomfield, Biophys. J. **74**, 3152 (1998).

[31] N. V. Hud and M. Polak, Curr. Opin. Struct. Biol. **11**, 293 (2001).

[32] A. K. Mazur and D. E. Kamashev, Phys. Rev. E **66**, 011917(1 (2002).

[33] A. Merling, N. Sagaydakova, and T. E. Haran, Biochemistry **42**, 4978 (2003).

[34] N. V. Hud and J. Plavec, Biopolymers **69**, 144 (2003).

[35] H.-S. Koo, J. Drak, J. A. Rice, and D. M. Crothers, Biochemistry **29**, 4227 (1990).

[36] N. B. Ulyanov and V. B. Zhurkin, J. Biomol. Struct. Dyn. **2**, 361 (1984).

[37] S. R. Sanghani, K. Zakrzewska, S. C. Harvey, and R. Lavery, Nucleic Acids Res. **24**, 1632 (1996).

[38] E. von Kitzing and S. Diekmann, Eur. Biophys. J. **14**, 13 (1987).

[39] V. P. Chuprina and R. A. Abagyan, J. Biomol. Struct. Dyn. **6**, 121 (1988).

[40] V. B. Zhurkin, N. B. Ulyanov, A. A. Gorin, and R. L. Jernigan, Proc. Natl. Acad. Sci. U.S.A. **88**, 7046 (1991).

[41] T. E. Cheatham, III and P. A. Kollman, Annu. Rev. Phys. Chem. **51**, 435 (2000).

[42] M. A. Young and D. L. Beveridge, J. Mol. Biol. **281**, 675 (1998).

[43] E. C. Sherer, S. A. Harris, R. Soliva, M. Orozco, and C. A. Laughton, J. Am. Chem. Soc. **121**, 5981 (1999).

[44] D. Strahs and T. Schlick, J. Mol. Biol. **301**, 643 (2000).

[45] A. K. Mazur, J. Am. Chem. Soc. **122**, 12778 (2000).

[46] A. K. Mazur, J. Biomol. Struct. Dyn. **18**, 832 (2001).

[47] J. D. Watson and F. H. C. Crick, Nature **171**, 737 (1953).

[48] M. D. Ediger, Annu. Rev. Phys. Chem. **51**, 99 (2000).

[49] L. Song and J. M. Schurr, Biopolymers **30**, 229 (1990).

[50] T. M. Okonogi, A. W. Reese, S. C. Alley, P. B. Hopkins, and R. H. Robinson, Biophys. J. **77**, 3256 (1999).

[51] E. B. Brauns, M. L. Madaras, R. S. Coleman, C. J. Murphy, and M. A. Berg, Phys. Rev. Lett. **88**, 158101 (2002).

[52] C. A. Thomas, Jr., J. Am. Chem. Soc. **78**, 1861 (1956).

[53] J. B. Hays and B. H. Zimm, J. Mol. Biol. **48**, 297 (1970).

[54] D. Shore and R. L. Baldwin, J. Mol. Biol. **170**, 957 (1983).

[55] C. H. Hsieh and J. D. Griffith, Proc. Natl. Acad. Sci. U.S.A. **86**, 4833 (1989).

[56] J. M. L. Pieters, R. M. W. Mans, H. van den Elst, G. A. van der Marel, J. H. van Boom, and C. Altona, Nucleic Acids Res. **17**, 4551 (1989).

[57] E. A. Snowden-Ifft and D. E. Wemmer, Biochemistry **29**, 6017 (1990).

[58] J. Aymami, M. Coll, G. A. van der Marel, J. H. van Boom, A. H.-J. Wang, and A. Rich, Proc. Natl. Acad. Sci. U.S.A. **87**, 2526 (1990).

[59] D. Rentzeperis, J. Ho, and L. A. Marky, Biochemistry **29**, 2564 (1993).

[60] E. Le Cam, F. Fack, J. Ménissier-de Murcia, J. A. H. Cognet, A. Barbin, V. Sarantoglou, B. Révet, E. Delain, and G. de Murcia, J. Mol. Biol. **235**, 1062 (1994).

[61] J. B. Mills, J. P. Kooper, and P. J. Hagerman, Biochemistry **33**, 1797 (1994).

[62] K. R. Hagerman and P. J. Hagerman, J. Mol. Biol. **260**, 207 (1996).

[63] P. Furrer, J. Bednar, A. Z. Stasiak, V. Katritch, D. Michoud, A. Stasiak, and J. Dubochet, J. Mol. Biol. **266**,

711 (1997).
[64] M. J. Lane, T. Paner, I. Kashin, B. D. Faldasz, B. Li, F. J. Gallo, and A. S. Benight, Nucleic Acids Res. **25**, 611 (1997).
[65] S. Singh, P. K. Patel, and R. H. Hosur, Biochemistry **36**, 13214 (1997).
[66] C. Roll, C. Ketterlé, V. Faibis, G. V. Fazakerley, and Y. Boulard, Biochemistry **37**, 4059 (1998).
[67] L. Kozerski, A. B. Mazurek, R. Kawecki, W. Bocian, P. Krajewski, E. Bednarek, J. Sitkowski, M. P. Williamson, A. J. G. Moir, and P. E. Hansen, Nucleic Acids Res. **29**, 1132 (2001).
[68] H. Kuhn, E. Protozanova, and V. V. Demidov, Electrophoresis **23**, 2384 (2002).
[69] W. D. Cornell, P. Cieplak, C. I. Bayly, I. R. Gould, K. M. Merz, D. M. Ferguson, D. C. Spellmeyer, T. Fox, J. W. Caldwell, and P. A. Kollman, J. Am. Chem. Soc. **117**, 5179 (1995).
[70] T. E. Cheatham, III, P. Cieplak, and P. A. Kollman, J. Biomol. Struct. Dyn. **16**, 845 (1999).
[71] W. L. Jorgensen, J. Am. Chem. Soc. **103**, 335 (1981).
[72] S. Arnott and D. W. L. Hukins, Biochem. Biophys. Res. Commun. **47**, 1504 (1972).
[73] A. K. Mazur, J. Comput. Chem. **18**, 1354 (1997).
[74] A. K. Mazur, in *Computational Biochemistry and Biophysics*, edited by O. M. Becker, A. D. MacKerell, Jr., B. Roux, and M. Watanabe (Marcel Dekker, New York, 2001), pp. 115–131.
[75] A. K. Mazur, J. Am. Chem. Soc. **120**, 10928 (1998).
[76] A. K. Mazur, J. Chem. Phys. **111**, 1407 (1999).
[77] A. K. Mazur, J. Phys. Chem. B **102**, 473 (1998).
[78] A. K. Mazur, B. G. Sumpter, and D. W. Noid, Comput. Theor. Polym. Sci. **11**, 35 (2001).
[79] A. K. Mazur, J. Comput. Chem. **22**, 457 (2001).
[80] L. Wang, B. E. Hingerty, A. R. Srinvasan, W. K. Olson, and S. Broyde, Biophys. J. **83**, 382 (2002).
[81] U. Essmann, L. Perera, M. L. Berkowitz, T. Darden, H. Lee, and L. G. Pedersen, J. Chem. Phys. **103**, 8577 (1995).
[82] T. E. Cheatham, III and M. A. Young, Biopolymers **56**, 232 (2000-2001).
[83] H.-S. Koo, H.-M. Wu, and D. M. Crothers, Nature **320**, 501 (1986).
[84] S. Diekmann and J. C. Wang, J. Mol. Biol. **186**, 1 (1985).
[85] S. Diekmann, Nucleic Acids Res. **15**, 247 (1987).
[86] R. Lavery and H. Sklenar, J. Biomol. Struct. Dyn. **6**, 63 (1988).
[87] W. Kabsch, C. Sander, and E. N. Trifonov, Nucleic Acids Res. **10**, 1097 (1982).
[88] R. E. Dickerson, M. Bansal, C. R. Calladine, S. Diekmann, W. N. Hunter, O. Kennard, R. Lavery, H. C. M. Nelson, W. K. Olson, W. Saenger, et al., J. Mol. Biol. **205**, 787 (1989).
[89] A. K. Mazur, J. Mol. Biol. **290**, 373 (1999).
[90] M. J. Packer and C. A. Hunter, J. Mol. Biol. **280**, 407 (1998).
[91] C. R. Calladine and H. R. Drew, *Understanding DNA: The Molecule & How it Works* (Academic Press, London, 1992).
[92] H. M. Berman, W. K. Olson, D. L. Beveridge, J. Westbrook, A. Gelbin, T. Demeny, S. H. Hsieh, A. R. Srinivasan, and B. Schneider, Biophys. J. **63**, 751 (1992).